2014 IEEE International Conference on Robotics & Automation (ICRA)
Hong Kong Convention and Exhibition Center
May 31 - June 7, 2014. Hong Kong, China

Auto-parametric resonance in cable-actuated systems

Jayender Bhardhwaj, Bin Yao and Arvind Raman

Abstract— **Cable-actuated systems provide an effective method for precise motion control over various distances. Motion control using such systems has traditionally focused on eliminating longitudinal resonances and disturbance. Moreover, longitudinal cable resonances are usually assumed to be at much higher frequencies compared to transverse resonances, ensuring minimal coupling between the two. However, in high-speed high-precision applications, the coupling between longitudinal and lateral cable oscillations cannot be ignored in the presence of high-inertia components. In this paper, we describe the mechanism of auto-parametric resonance in cable-pulley systems through which longitudinal vibrations can couple strongly to transverse vibrations. We model exact dynamics of coupled cable-pulley oscillations and solve them numerically to observe the intrinsic non-linear behavior. Preliminary experimental results show the effect of this coupling on pulley rotation.**

I. Introduction

Cable-actuated systems are increasingly used in a variety of devices such as remote telemanipulators [1], rehabilitative robotic devices and micro air vehicles [2]. They are also used in transporter systems such as high-rise elevators [3] and cranes. As the need for high speed and accuracy increases, precise motion control of these systems becomes necessary.

Research efforts on motion control of cable-actuated systems focus on suppression of either longitudinal or transverse vibrations individually while ignoring the coupling between them. Longitudinal vibrations in cable transporter systems have been studied in [3]-[5]. In [3], the theory of δ-flatness is used to describe the input-output behavior using a differential-difference equation and an open-loop controller is designed to dampen longitudinal vibrations and get minimal residual motion of the transported object. In [4],[5], the exact infinite-dimensional model of the system is approximated using a finite-dimensional model. Robust controllers are designed to remove longitudinal vibration energy from the system and reduce the fundamental resonance peak. Control of transverse vibrations have been more widely studied in cable-actuated systems [6]-[8] and axially moving cable systems [9],[10]. While active control schemes have been shown to improve desired performance, both passive and active control have been proposed with a focus on stabilizing the system by dampening the transverse vibrations through energy dissipation. In many of these cable-actuated motion control applications including those that contain high-inertia components, longitudinal and lateral cable vibrations are considered to be uncoupled and the reduction in fundamental longitudinal frequency is not calculated. Under certain conditions, this coupling can manifest in the form of auto-parametric excitation leading to loss of performance.

The goals of this paper are (1) to explain the occurrence of intrinsic parametric resonance in cable-pulley systems that causes strong coupling between longitudinal and transverse cable oscillations and (2) to show its effect on motion output. The rest of the paper is organized as follows. First, the exact, non-planar, coupled governing equations for stretched cable vibrations are derived. They are then combined with appropriate dynamic boundary conditions and pulley dynamics to fully describe the cable-pulley system. The effect of high-inertia components such as the pulleys, on the fundamental longitudinal frequency of the cable is examined, through modal analysis of the linearized cable dynamics. Following this, the condition for auto-parametric resonance is explored through a parametric analysis of the system. The exact non-linear coupled cable vibrations are numerically simulated to show the occurrence of auto-parametric resonance and its effect on motion output.

II. Exact governing equations

A. Cable Dynamics

The modeling of cable or string vibrations has been extensively studied in literature. Classical derivations of the linear wave equation can be found in [13], where assumptions included planar motion, small displacements, slopes and changes in tension. Equations for coupled non-linear cable vibrations can be found in [15]-[19]. In many cases transverse coupling was considered and longitudinal motion was ignored. Transverse-longitudinal vibration coupling has been studied in [20]-[23], though no exact solutions were found. In general, different governing equations have been derived for vibrations of strings due to the different assumptions made. In this section, the exact coupled non-planar dynamics of a

The authors are with the School of Mechanical Engineering, Purdue University, West Lafayette, IN 47907, USA (jbhardhw, byao, raman@purdue.edu).

Bin Yao is also a Chang Jiang Chair Professor at the State Key Laboratory of Fluid Power Transmission and Control of Zhejiang University in China (on leave from Purdue University), supported in part by the Science Fund for Creative Research Groups of National Natural Science Foundation of China (No: 51221004).

stretched cable are derived making only the assumption that Hooke's law is valid.

We first consider an un-stretched cable segment of length dl that is stretched to length dx to produce a constant pretension T_0. We represent this pre-stretched element of length dx by the segment AB as shown in Fig. 1. The pre-strain in the element can hence be calculated as the ratio of change in length to original length,

$$\epsilon_0 = \frac{dx - dl}{dl} = \frac{dx}{dl} - 1 \tag{1}$$

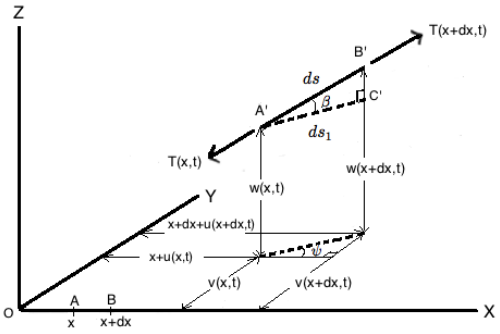

Fig. 1. Cable element stretched during vibration

During operation of the cable-pulley system, the segment AB of length dx changes further to the segment $A'B'$ of length ds as shown in Fig. 1. We will assume AB to be along the X axis with A at coordinates (x, y, z) and B at coordinates $(x + dx, y, z)$. We define the displacements of point A parallel to the X, Y and Z axes to be $u(x,t)$, $v(x,t)$ and $w(x,t)$ respectively. Similarly, the displacements of point B are $u(x+dx,t)$, $v(x + dx, t)$ and $w(x + dx, t)$. The stretched cable segment length ds is given by,

$$ds = dx\sqrt{(1+u')^2 + v'^2 + w'^2} \tag{2}$$

Hence the net strain can be calculated as,

$$\epsilon(x,t) = \epsilon_0 + (1+\epsilon_0)(\sqrt{(1+u')^2 + v'^2 + w'^2} - 1) \tag{3}$$

where the primes denote partial differentiation with respect to x. From Hooke's law, the expression for net tension in the cable at the point originally at x is given by,

$$T(x,t) = T_0 + EA(1+\epsilon_0)(\sqrt{(1+u')^2 + v'^2 + w'^2} - 1) \tag{4}$$

where E is young's modulus of the cable material, A is the area of cross section and ρ is the static linear mass density. Assuming no damping forces, the dynamics of the cable element are given by equating the net tension force in each direction to the rate of change of momentum [15],

$$\begin{aligned} \rho\ddot{u}(x,t) &= \frac{\partial T_x}{\partial x} \\ \rho\ddot{v}(x,t) &= \frac{\partial T_y}{\partial x} \\ \rho\ddot{w}(x,t) &= \frac{\partial T_z}{\partial x} \end{aligned} \tag{5}$$

Substituting for the components of tension from Fig. 1, we get the following coupled non-linear cable dynamics.

$$\begin{aligned} \ddot{u}(x,t) = &\frac{u''c_w^2 + c_u^2(1+u')\frac{(1+u')u'' + v'v'' + w'w''}{\sqrt{(1+u')^2+v'^2+w'^2}}}{\sqrt{(1+u')^2 + v'^2 + w'^2}} \\ &+ \frac{c_u^2 u''(\sqrt{(1+u')^2 + v'^2 + w'^2} - 1)}{\sqrt{(1+u')^2 + v'^2 + w'^2}} \\ &- \frac{\frac{(1+u')((1+u')u'' + v'v'' + w'w'')(c_w^2 + c_u^2(\sqrt{(1+u')^2+v'^2+w'^2}-1))}{((1+u')^2+v'^2+w'^2)}}{\sqrt{(1+u')^2 + v'^2 + w'^2}} \end{aligned} \tag{6}$$

$$\begin{aligned} \ddot{v}(x,t) = &\frac{v''c_w^2 + c_u^2 v'\frac{(1+u')u'' + v'v'' + w'w''}{\sqrt{(1+u')^2+v'^2+w'^2}}}{\sqrt{(1+u')^2 + v'^2 + w'^2}} \\ &+ \frac{c_u^2 v''(\sqrt{(1+u')^2 + v'^2 + w'^2} - 1)}{\sqrt{(1+u')^2 + v'^2 + w'^2}} \\ &- \frac{\frac{v'((1+u')u'' + v'v'' + w'w'')(c_w^2 + c_u^2(\sqrt{(1+u')^2+v'^2+w'^2}-1))}{((1+u')^2+v'^2+w'^2)}}{\sqrt{(1+u')^2 + v'^2 + w'^2}} \end{aligned} \tag{7}$$

$$\begin{aligned} \ddot{w}(x,t) = &\frac{w''c_w^2 + c_u^2 w'\frac{(1+u')u'' + v'v'' + w'w''}{\sqrt{(1+u')^2+v'^2+w'^2}}}{\sqrt{(1+u')^2 + v'^2 + w'^2}} \\ &+ \frac{c_u^2 w''(\sqrt{(1+u')^2 + v'^2 + w'^2} - 1)}{\sqrt{(1+u')^2 + v'^2 + w'^2}} \\ &- \frac{\frac{w'((1+u')u'' + v'v'' + w'w'')(c_w^2 + c_u^2(\sqrt{(1+u')^2+v'^2+w'^2}-1))}{((1+u')^2+v'^2+w'^2)}}{\sqrt{(1+u')^2 + v'^2 + w'^2}} \end{aligned} \tag{8}$$

$c_u^2 = \frac{EA(1+\epsilon_0)}{\rho}$ and $c_w^2 = \frac{EA\epsilon_0}{\rho}$ are longitudinal and lateral wave velocities respectively. Gravity will be included once a coordinate system specific to the cable-pulley setup has been defined.

The cable-pulley setup shown in Fig. 2 is in its un-stretched configuration. Hence the distance between the pulleys is L. Two separate yet related coordinate systems have been defined. X_1, Y_1, Z_1 is fixed at the first point of contact between the pulley on the left and the upper cable. Similarly, X_2, Y_2, Z_2 is fixed at the first point of contact between the pulley on the right and the lower cable. Both X_1 and X_2 directions are along the cable

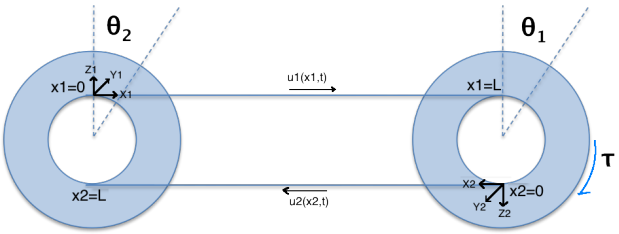

Fig. 2. Cable-pulley system

lengths. Using these coordinate systems, (6)-(8) can be rewritten as,

$$\begin{aligned}\ddot{u}_1(x_1,t) &= F(u_1,v_1,w_1,u_1',v_1',w_1',u_1'',v_1'',w_1'')\\ \ddot{v}_1(x_1,t) &= G(u_1,v_1,w_1,u_1',v_1',w_1',u_1'',v_1'',w_1'')+g\\ \ddot{w}_1(x_1,t) &= H(u_1,v_1,w_1,u_1',v_1',w_1',u_1'',v_1'',w_1'')\end{aligned} \quad (9)$$

and

$$\begin{aligned}\ddot{u}_2(x_2,t) &= F(u_2,v_2,w_2,u_2',v_2',w_2',u_2'',v_2'',w_2'')\\ \ddot{v}_2(x_2,t) &= G(u_2,v_2,w_2,u_2',v_2',w_2',u_2'',v_2'',w_2'')+g\\ \ddot{w}_2(x_2,t) &= H(u_2,v_2,w_2,u_2',v_2',w_2',u_2'',v_2'',w_2'')\end{aligned} \quad (10)$$

Other than the assumption that cable strain is small enough for Hooke's law (4) to be valid, these governing equations are exact. Equation (4) can be replaced by a more realistic non-linear stress-strain relation in future studies.

B. Pulley dynamics

The setup in Fig. 2 is in a pull-pull configuration with both cables attached to the two pulleys on each end. The motion of the pulleys is governed by,

$$\begin{aligned}I_1\ddot{\theta}_1 + c_1\dot{\theta}_1 &= \big(T_1(0,t) - T_2(L_e,t)\big)r_1\\ I_2\ddot{\theta}_2 + c_2\dot{\theta}_2 &= \big(T_2(0,t) - T_1(L_e,t)\big)r_2\end{aligned} \quad (11)$$

$L_e = L(1+\epsilon_0)$ is the cable length between the pulleys after pre-stretching. Equation (11) describes the free motion of the two pulleys (τ=0). It can be seen that the pulley dynamics is coupled with the cable vibrations through cable tension which which is a time-varying function of cable strain.

C. Boundary conditions

Since the cables ends are attached to the pulleys, their displacements are constrained by the rotation of the pulleys. Hence the boundary conditions for the cables are given by,

$$\begin{aligned}&u_1(0,t) = u_2(L_e,t) = r_1\theta_1(t)\\ &u_1(L_e,t) = u_2(0,t) = r_2\theta_2(t)\\ &v_1(0,t) = v_1(L_e,t) = v_2(0,t) = v_2(L_e,t) = 0\\ &w_1(0,t) = w_1(L_e,t) = w_2(0,t) = w_2(L_e,t) = 0\end{aligned} \quad (12)$$

The system defined by (9)-(12) can be simulated to understand the effect of cable vibrations on pulley performance.

III. Reduced Longitudinal Frequency

In order to calculate the effect of high-inertia components in the system on cable vibrations, a modal analysis of the linear cable dynamics is performed and the following approximations are made,

$$\begin{aligned}u'^2, v'^2, w'^2 &<< u'\\ u' &<< 1\end{aligned} \quad (13)$$

Under these assumptions the strain and tension at any point in the string can be simplified from (3) and (4) to give,

$$\begin{aligned}\epsilon(x,t) &= \epsilon_0 + (1+\epsilon_0)u'(x,t)\\ T(x,t) &= T_0 + EA(1+\epsilon_0)u'(x,t)\end{aligned} \quad (14)$$

Equations (6)-(8) can also be de-coupled as shown.

$$\begin{aligned}\ddot{u}(x,t) &= c_u^2 u''(x,t)\\ \ddot{v}(x,t) &= c_w^2 v''(x,t)\\ \ddot{w}(x,t) &= c_w^2 w''(x,t)\end{aligned} \quad (15)$$

For standard modal analysis we look for separable solutions to $u(x,t)$ in the form $u(x,t) = B(x)A(t)$. Substituting it in the longitudinal dynamics in (15), we get

$$\begin{aligned}B(x)\ddot{A}(t) &= c_u^2 B''(x)A(t)\\ c_u^2\frac{B''(x)}{B(x)} &= \frac{\ddot{A}(t)}{A(t)} = -\omega^2\\ B(x) &= b_1\sin(\frac{\omega x}{c_u}) + b_2\cos(\frac{\omega x}{c_u})\\ \text{and } A(t) &= a_1\sin(\omega t) + a_2\cos(\omega t)\end{aligned} \quad (16)$$

where $\frac{\omega}{2\pi}$ will represent natural longitudinal frequencies. Applying the boundary conditions in (12) to (16),

$$\begin{aligned}r_1\theta_1(t) &= b_2(a_1\sin(\omega t) + a_2\cos(\omega t))\\ r_2\theta_2(t) &= \left(b_1\sin(\frac{\omega L_e}{c_u}) + b_2\cos(\frac{\omega L_e}{c_u})\right).\\ &\quad (a_1\sin(\omega t) + a_2\cos(\omega t))\end{aligned} \quad (17)$$

Differentiating (17), we get

$$\begin{aligned}r_1\ddot{\theta}_1(t) &= -b_2\omega^2(a_1\sin(\omega t) + a_2\cos(\omega t))\\ r_2\ddot{\theta}_2(t) &= -\omega^2\left(b_1\sin(\frac{\omega L_e}{c_u}) + b_2\cos(\frac{\omega L_e}{c_u})\right).\\ &\quad (a_1\sin(\omega t) + a_2\cos(\omega t))\end{aligned} \quad (18)$$

From pulley dynamics (11), in the absence of damping we get

$$\begin{aligned}\frac{I_1}{r_1}\ddot{\theta}_1(t) &= T_1(0,t) - T_2(L_e,t)\\ &= EA(1+\epsilon_0)(u_1'(0,t) - u_2'(L_e,t))\\ &= 2EA(1+\epsilon_0)u_1'(0,t)\\ &= 2EA(1+\epsilon_0)\frac{\omega b_1}{c_u}(a_1\sin(\omega t) + a_2\cos(\omega t))\\ \frac{I_2}{r_2}\ddot{\theta}_2(t) &= T_2(0,t) - T_1(L_e,t)\\ &= EA(1+\epsilon_0)(u_2'(0,t) - u_1'(L_e,t))\\ &= -2EA(1+\epsilon_0)u_1'(L_e,t)\\ &= -2EA(1+\epsilon_0)\frac{\omega}{c_u}(a_1\sin(\omega t) + a_2\cos(\omega t)).\\ &\quad\left(b_1\cos(\frac{\omega L_e}{c_u}) - b_2\sin(\frac{\omega L_e}{c_u})\right) \qquad (19)\end{aligned}$$

From (18) and (19), we get

$$\frac{\omega_n I_2}{2c_u\rho r_2^2} = \frac{\frac{-\omega_n I_1}{2c_u\rho r_1^2}\cos(\frac{\omega_n L_e}{c_u}) - \sin(\frac{\omega_n L_e}{c_u})}{\frac{-\omega_n I_1}{2c_u\rho r_1^2}\sin(\frac{\omega_n L_e}{c_u}) + \cos(\frac{\omega_n L_e}{c_u})} \qquad (20)$$

Characteristic equation (20) has infinitely many solutions, $\omega_n, n = 0, 1, 2...$ and is solved for numerically using Matlab's 'fzero' function. Fig. 3 shows the Fast Fourier Transform of the experimentally recorded free oscillations of the cable-pulley system, using nylon pulleys monofilament steel cables of diameter $0.01in$. The peak matches closely with the theoretical fundamental longitudinal frequency of 81.73 Hz obtained from (20).

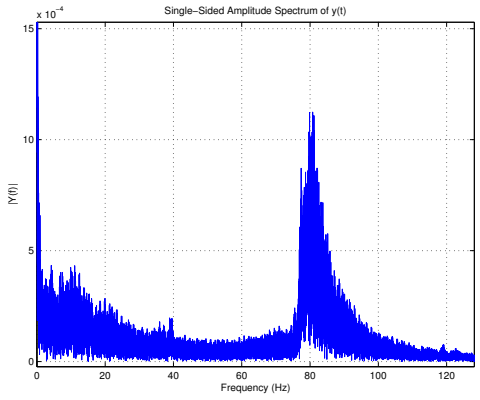

Fig. 3. FFT of cable-pulley system's free oscillations ($L = 1m, T_0 = 2.6N, r_1 = r_2 = 3cm$)

IV. Auto-Parametric Resonance

Parametric excitation of string vibrations was first treated theoretically by Lord Rayleigh [24] who showed that if the tension of the wire is varied periodically using an external input, at twice one of its mode frequencies, then the system is unstable and oscillations grow. More theoretical and experimental work can be found in [25]-[29]. In our current work, we show that the behavior studied by Lord Rayleigh is intrinsic to cable-pulley systems, where the periodic variation of tension is due to the fundamental longitudinal vibration of the cable. Since this frequency is reduced by high-inertia components in the system, auto-parametric resonance is expected to occur when the following condition is satisfied.

$$\omega_{lateral} : \omega_{longitudinal} = 1 : 2 \qquad (21)$$

A. Parametric Analysis

In order to predict when auto-parametric resonance occurs in the cable-pulley system, we take a closer look at (20) which relates the reduced fundamental longitudinal frequency of the system, to all the physical parameters of the cable and pulleys. The fundamental lateral vibration frequency is given by $f_{lateral} = \frac{c_w}{2L_e}$. If $\gamma = \frac{f_{lateral}}{\omega_n/2\pi} = \frac{\pi c_w}{\omega_n L_e}$ is the ratio of fundamental lateral frequency to longitudinal frequency and $\chi_1 = \frac{I_1}{2\rho r_1^2 L_e}$, $\chi_2 = \frac{I_2}{2\rho r_2^2 L_e}$, then (20) can be re-written as,

$$\frac{\pi c_w}{\gamma c_u}\chi_2 = \frac{\frac{-\pi c_w}{\gamma c_u}\chi_1\cos(\frac{\pi c_w}{\gamma c_u}) - \sin(\frac{\pi c_w}{\gamma c_u})}{\frac{-\pi c_w}{\gamma c_u}\chi_1\sin(\frac{\pi c_w}{\gamma c_u}) + \cos(\frac{\pi c_w}{\gamma c_u})} \qquad (22)$$

χ_1 and χ_2 are essentially mass ratios of each pulley to total cable and can be treated as non-dimensional quantities representative of different cable-pulley systems.

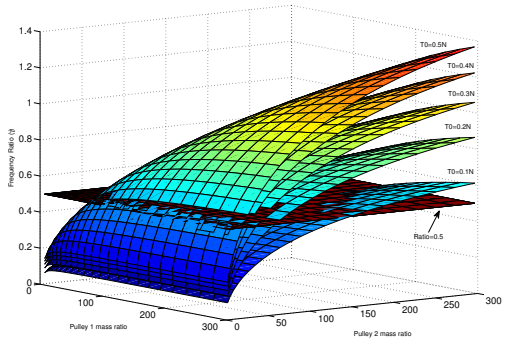

Fig. 4. Variation of cable vibration frequency ratio (γ) with mass ratios (χ_1 and χ_2) for a different cable pre-tensions.

The surfaces in Fig. 4 represent different cable pre-tensions while the plane represents a constant frequency ratio of 0.5. The intersection of the plane with the surfaces gives a family of curves that correspond to auto-parametric resonance in the cable-pulley system.

V. Numerical & Experimental Results

The cable-pulley system shown in Fig. 2 and represented by (9)-(12), is numerically simulated using a central difference scheme in time and space. It provides

an explicit solution to the cable-pulley vibrations and as a result, a CFL number less than unity was chosen for numerical stability. The two pulleys are initially assumed to be at rest. While gravity acts in the Y direction, the nylon cables are given triangular perturbations at $t = 0$ with maximum displacements at their midpoints. This is equivalent to plucking the cables such that the following initial conditions are used.

$$\begin{aligned} u_1(L_e/2, 0) &= 10^{-4}m, \; u_2(L_e/2, 0) = -10^{-4}m \\ v_1(L_e/2, 0) &= 10^{-4}m, \; v_2(L_e/2, 0) = 10^{-4}m \\ w_1(L_e/2, 0) &= 10^{-4}m, \; w_2(L_e/2, 0) = 10^{-4}m \end{aligned} \quad (23)$$

Fig. 5 shows strong coupling between the two transverse and longitudinal vibrations at the cable midpoint, as well as free rotation of one of the pulleys, when condition (21) is satisfied. Fig. 6 shows the oscillations of the cable midpoint and the pulley for the same initial conditions, using linear uncoupled cable dynamics. Compared to the uncoupled vibrations, the coupled vibrations show larger oscillations of the pulley.

Fig. 7 shows data obtained experimentally using monofilament steel cables along with other system parameters that satisfy (21). The coupling between transverse cable vibrations and pulley oscillations can be observed over the first second after which the effect of cable damping becomes prominent.

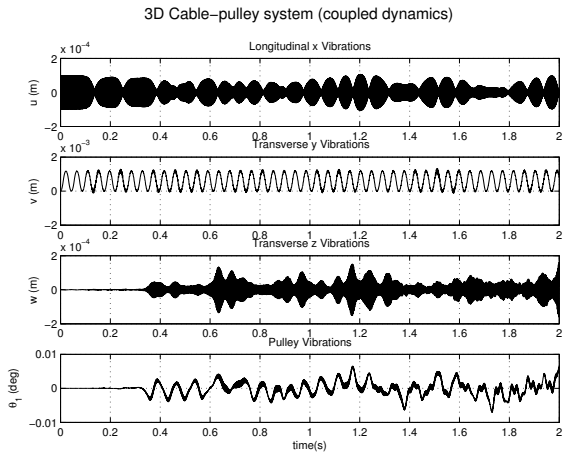

Fig. 5. Coupled vibrations of cable midpoint in the longitudinal and two transverse directions is shown in the first three plots. The last plot shows pulley oscillations.

A. Code Verification

The Richardson extrapolation process is used to eliminate the highest-order error terms in a discrete solution, to get closer to the exact numerical solution [30]. Since it does not depend on a specific numerical method used to obtain that solution, it can be used as a post-processing procedure. Assuming that the discrete solution $F(h)$ is a

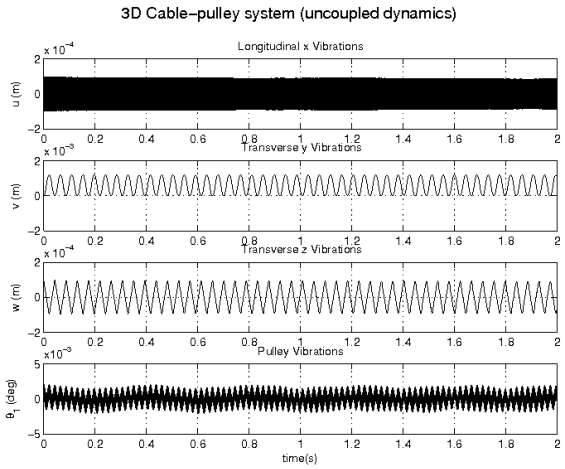

Fig. 6. Vibrations of cable midpoint and pulley using linear cable dynamics.

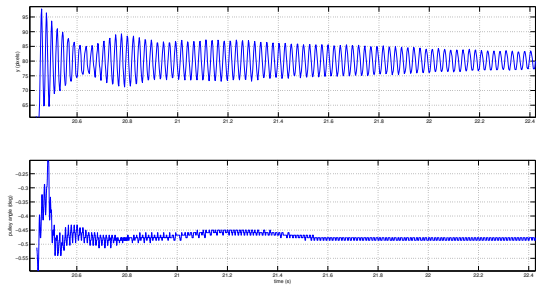

Fig. 7. Observed transverse vibrations of cable midpoint (top) and pulley oscillations (bottom) showing coupling.

continuous and differentiable function of a representative spatial grid size h, we have the following equations in the asymptotic range [31],

$$F_{exact} - F_1 = C(h/r_1)^n \quad (24)$$
$$F_{exact} - F_2 = C(h/r_2)^n \quad (25)$$
$$F_{exact} - F_3 = C(h/r_3)^n \quad (26)$$

n is the apparent order of the numerical method, F_{exact} is the numerically exact solution corresponding to zero grid size, r_1, r_2 and r_3 are grid refinement factors defined as the ratio of grid sizes $r_i = h_{ref}/h_i$. Without loss of generality, we assume $r_1 = 1$ and make that the reference grid. Combining (24) and (25) to eliminate the leading error term, we get the Richardson extrapolation for the discrete solution on two different grids as,

$$RE^n(F_1, F_2) = \frac{F_2 r_2^n - F_1}{r_2^n - 1} + O(h^{n+1}) \quad (27)$$

Combining solutions from all three grids in (24)-(26) to eliminate two leading error terms, we get

$$RE^n(F_1,F_2,F_3) = \frac{\alpha_3 RE^n(F_1,F_2) - \alpha_2 RE^n(F_1,F_3)}{\alpha_3 - \alpha_2} + O(h^{n+2}) \tag{28}$$

where $\alpha_i = \frac{r_i - 1}{r_i(r_i^n - 1)}$. Replacing F by cable vibration amplitude u, the numerical error can be calculated from (28). The approximate relative error in u from a mesh with grid size h is $\epsilon = \frac{RE - u(h)}{RE}$. Table I shows maximum cable vibration amplitude and grid refinement factors for different uniform grids, along with approximate relative errors. $RE^2(161, 221, 261)$ was used as the exact solution for u_{max}. The numerical error is less than 5% for meshes with 201 grid points or more. In all simulations, 201 grid points were used.

TABLE I
CALCULATED MAXIMUM DISPLACEMENT

Grid points	r	u_{max}	$error\ \epsilon, \%$
161	1	9.191×10^{-5}	5.48
201	1.25	9.240×10^{-5}	4.97
221	1.375	9.313×10^{-5}	4.22
261	1.625	9.392×10^{-5}	3.41
$RE^2(161, 221)$	-	9.45×10^{-5}	2.82
$RE^2(161, 261)$	-	9.5142×10^{-5}	2.16
$RE^2(221, 261)$	-	9.5904×10^{-5}	1.37
$RE^2(161, 221, 261)$	-	9.7238×10^{-5}	

VI. CONCLUSION

Experiments on a cable-pulley system confirm a reduction in fundamental longitudinal frequency due to the inertia of the pulleys. This reduction allows coupling between longitudinal and lateral vibration modes that are usually thought to be decoupled. Simulation results of exact cable-pulley dynamics under conditions of autoparametric resonance show strong coupling between longitudinal and lateral cable vibrations. Preliminary experimental results also show the effect of this coupling on pulley oscillations, making it an interesting design/control problem for motion control applications.

REFERENCES

[1] A.G. Smith and J.R. Hewit, Control of an experimental robot arm with non-ideal transmission elements, *IEEE Intl. Workshop on Intelligent Motion Control*, 1990, pp. 485-490.

[2] M. Keennon, K. Klingebiel, H. Won, A. Andriukov, Development of the Nano Hummingbird: A Tailless Flapping Wing Micro Air Vehicle, 50th AIAA Aero. Sc. Meeting, Jan 2012.

[3] S.K. Agrawal, H.R. Pota, Y. Zhang, A flatness based approach to trajectory modification of residual motion of cable transporter systems, Proc. Am. Control Conf., vol. 2, pp. 1587-1592, 2001.

[4] Y. Zhang, S.K. Agrawal, H.R. Pota and I.R. Petersen, Minimax linear quadratic gaussian control of longitudinal vibration for cable transporter systems with multiplicative nonparametric uncertainties, *Intl. J. Acoust. Vib.*, vol. 10, No. 3, pp. 1-7, 2005.

[5] Y. Zhang, S.K. Agrawal, P. Hagedorn, Longitudinal vibration modeling and control of flexible transporter system with arbitrarily varying cable lengths, *J. Vib. Control*, vol. 11, no. 3, pp. 431-456, 2005.

[6] C.F. Baicu, C.D. Rahn, B.D. Nibali, Active boundary control of elastic cables: Theory and experiment, *J. Sound Vib.*, vol. 198, no. 1, pp. 17-26, 1996.

[7] H. Canbolat, D. Dawson, C. Rahn, S. Nagarkatti, Adaptive boundary control of out-of-plane cable vibration, *J. Applied Mechanics*, vol. 65, pp. 963-969, 1998.

[8] Y. Zhang, S.K. Agrawal, Lyapunov controller design for transverse vibration of a cable-linked transporter system, *Multibody System Dynamics*, vol. 15, pp. 287-304, 2006.

[9] J.A. Wickert, C.D. Mote, Classical vibration analysis of axially moving continua, *Transactions of ASME*, vol. 57, pp. 738-744, 1990.

[10] S.M. Shahruz, D.A. Kurmaji, Vibration suppression of non-linear axially moving string by boundary control, *J. Sound Vib.*, vol. 201, no. 1, pp. 145-152, 1997.

[11] Q.C Nguyen, K-S Hong, Asymptotic stabilization of a nonlinear axially moving string by adaptive boundary control, *J. Sound Vib.*, vol. 329, pp. 4588-4603, 2010.

[12] L. Lu, Z. Chen, B. Yao, Q. Wang, A two-loop performance-oriented tip tracking control of a linear motor driven flexible beam system with experiments, *IEEE Trans. Industrial Electronics*, vol. 3, no. 3, 2011

[13] C.A. Coulson and A. Jeffrey, *Waves*, 2 ed. London: Longman, 1977.

[14] P.M. Morse and K.U. Ingard, *Theoretical Acoustics*, New York: McGraw-Hill, 1968.

[15] G.F. Carrier, On the non-linear vibration problem of the elastic string, *Q. Appl. Math*, vol. 3, pp. 157-165, 1945.

[16] E.W. Lee, Non-linear forced vibration of a stretched string, *Br.J. Appl. Phys.*, vol. 8, pp. 411-413, 1957.

[17] G.S.S. Murthy and B.S. Ramakrishna, Non-linear character of resonance in stretched strings, *J. Acoust. Soc. Am.*, vol. 38, pp. 461-471, 1967.

[18] J.A. Elliot, Intrinsic nonlinear effects in vibrating strings, *Am. J. Phys.*, vol. 48, no. 6, pp. 478-480, 1980.

[19] H.P.W. Gottlieb, Non-linear, non-planar transverse free vibration of a constant-tension string, *J. Sound Vib.*, vol. 191, no. 4, pp. 563-575, 1996.

[20] R. Narasimha, Non-linear vibration of an elastic string, *J. Sound Vib.*, vol. 8, no. 1, pp. 134-146, 1968.

[21] E.V. Kurmychev, Transverse and longitudinal mode coupling in a free vibrating soft string, *Physics Letters A* 310, pp. 148-160, 2003.

[22] A. Watzky, On the nonlinear models of the vibrating string, *J. Acoust. Soc. Am.*, vol. 118, no. 3, pp. 1973, 2005.

[23] Y. Zhang and S. Agrawal, Coupled vibrations of a varying length flexible cable transporter system with arbitrary axial velocity, Proc. Am. Control Conf., 2004.

[24] J.W. Strutt, On maintenance of vibrations by forces of double frequency and on the propagation of waves through a medium endowed with periodic structure, *Philosophical Magazine*, vol. 24, pp. 145-159, 1887.

[25] A. Stephenson, On a class of forced oscillations, *Q. J. Math*, vol. 37, pp. 353-360, 1906.

[26] J.A. Elliot, Nonlinear resonance in vibrating strings, *Am. J. Phys.*, vol. 50, no. 12, pp. 1148-1150, 1982.

[27] G.V. Rao and R.N. Iyengar, Internal Resonance and Non-linear Response of a Cable Under Periodic Excitation, *J. Sound. Vib.*, vol. 149, no. 1, pp. 25-41, 1991.

[28] Y. Fujino, P. Warnitchai, B.M. Pacheco, An experimental and analytical study of autoparametric resonance in a 3DOF model of cable-stayed-beam, *Nonlinear Dynamics*, vol. 4, no. 2, pp. 111-138, 1993.

[29] A. Tondl, *Autoparametric Resonance in Mechanical Systems*, Cambridge University Press, 2000.

[30] I. Celik and W.-M. Zhang, Calculation of numerical uncertainty using Richardson Extrapolation: Application to some simple turbulent flow calculations, *J. Fluids Engineering, Transactions of ASME*, vol. 117, no. 3, pp. 439-435, 1995.

[31] A.A. Alexeenko, Numerical Error Analysis for Deterministic Kinetic Solutions of Low-Speed Flows, Proc. 25th Intl. Symposium on Rarefied Gas Dynamics, St. Petersburg, Russia, 2006.